Computers in Biology and Medicine 111 (2019) 103326

Contents lists available at ScienceDirect

Computers in Biology and Medicine

journal homepage: www.elsevier.com/locate/compbiomed

An automated computer vision based preliminary study for the identification of a heavy metal (Hg) exposed fish-*channa punctatus*

Ashish Issac[a], Arti Srivastava[b], Ashutosh Srivastava[c], Malay Kishore Dutta[d,*]

[a] Department of Electronics & Communication Engineering, Amity University Uttar Pradesh, Noida, India
[b] Amity Institute of Biotechnology, Amity University Uttar Pradesh, Noida, India
[c] Amity Institute of Marine Science and Technology, Amity University Uttar Pradesh, Noida, India
[d] Centre for Advanced Studies, Dr. APJ Abdul Kalam Technical University, Lucknow, India

ARTICLE INFO

Keywords:
Image processing
Fish
Eyes
Heavy metal exposure
Circular hough transform
Adaptive intensity threshold
Mathematical morphology
Colour space transformation

ABSTRACT

Fishes available in the market may be cultured either in fresh or contaminated water bodies. Heavy metals are one of those contaminants which may cause menace to fish health and thereby affect the health of living beings consuming them. The identification of heavy metal residues in fish samples is a challenging task and may require expensive and sophisticated instruments and testing. This paper investigates visual changes which may be used as benchmark for differentiating between fresh water and heavy metal exposed fishes. The proposed method is an automated non-destructive image processing method for identifying visual changes which can be used to differentiate between controlled (untreated) and heavy metals exposed (treated) fishes. The eye of the fish from digital images is considered as focal tissue that was automatically segmented using the Circular Hough Transform and adaptive intensity thresholding. Post segmentation, a potential feature is identified and transformed into mathematical parameters for classification of a fish sample as fresh or heavy metal exposed water fish. The proposed method can identify and translate the potential visual feature for ease of understanding. The accuracy of the proposed method is high, and computation time elapsed indicates the possibility of using such algorithm for real time detection in related field.

1. Introduction

Fish is a vital source of food and rich source of animal protein for people around the world. 30% of the animal protein requirement in developing country has been fulfilled by fish. Consumption of fish as a food is increasing day by day due to awareness about its health benefits. Their consumption reduces many chronic non-communicable diseases [25]). However, many natural and anthropogenic activities are contaminating our waterbodies with various pollutants such as heavy metals [9]). Heavy metal contamination in aquatic ecosystem has become a global concern and a challenging environmental issue due to their adverse effects on human health [23].

Ubiquitous distribution and non-biodegradable nature of mercury (Hg) make it as one of the most hazardous pollutant that pose a serious threat to the living system [18]. Mercury contamination results primarily from various industrial activities including the mining, an alloy of mercury used for dental filling, various paints, consumer batteries and skin lightning creams [5,10,13]. The discharge of these persistent pollutants into water bodies results in the progressive and irreversible accumulation into the tissues of various aquatic species even if present at low concentration [17]. Transfer of these toxic metals in human through food chain is very common.

Several previous studies showed that contaminated fishes are the significant sources of mercury poisoning in humans [25,19]. In humans, various symptoms like anxiety, insomnia, memory impairment, and other nervous system related problems such as peripheral neuropathy, loss of peripheral vision, tremors in coordination, and depression are due to the mercury toxicity [13,2,6,28].

The use of computer vision techniques to impart fast and cost-effective solutions to real-time scenarios has become need of the hour and is also prevalent these days. Computer vision techniques have been employed to design a framework capable enough of assessing the quality of fish samples during the post harvesting phase. This solution may help consumers in identifying the freshness and classifying it into classes, such as fresh, moderately fresh and stale, depending on the number of days post harvestation [7,8]. Image processing methods have

* Corresponding author.
E-mail addresses: issac017@gmail.com (A. Issac), asrivastava@amity.edu (A. Srivastava), asrivastava4@amity.edu (A. Srivastava), malaykishoredutta@gmail.com (M.K. Dutta).

https://doi.org/10.1016/j.compbiomed.2019.103326
Received 7 January 2019; Received in revised form 7 June 2019; Accepted 11 June 2019

also been employed to assess the fish quality after exposure to pesticides, such as cypermethrin, which can be easily found in water sources [7,8].

Many researchers have worked in the domain of biomarker identification which can be used to assess relevant information from test sources. A protocol has been laid for identification of biomarkers to assess fish health in coastal areas and marine ecosystems [16]. Pathologies in liver and gills of the fishes have been detected and supported with the help of biochemical and genetic damages. These signs have been used as biomarkers to evaluate the potential effects of pollutants on aquatic life [26]. A similar study was performed on African catfish by analysing the effects of two different metabolic enzymes on its liver and gills. Some remarkable changes were observed in the selected organs of the sample fishes [22].

The main contribution of the proposed work lies in the identification of a potential visual feature which can be used to differentiate between a healthy and safe fish *(channa punctatus)* and a heavy metal (mercury) exposed one. Heavy metal exposure is responsible for the oxidative stress in fish. Several studies in higher vertebrates [11,21]; reviewed in Ref. [20] indicate that melanin synthesis is negatively affected by oxidative stress. In present study, heavy metal induced oxidative stress affects the melanin production which is more visible around the eye due to its thinness. This change may act as biomarker for the heavy metal toxicity in fish. This potential visual change near eye region, is converted to a mathematical parameter and represented as an angle subtended by an arc at the centre of a circle. This transformation seems appropriate and suits the algorithm as discrimination in values of both classes are observed.

Another significant contribution of the proposed work is its ability to correctly detect the eye region and its boundary even in the presence of reflections which gets introduced during the acquisition process. Post-harvesting, fish body secretes mucus, which prevents it from deterioration. This mucus accumulates on the scales of fish body and becomes a major cause of the reflection when light is thrown at it. Such reflections appear as bright dots on the surface of fish body which can hamper the accuracy of eye segmentation. With the help of statistical features, Circular Hough Transform, Intensity threshold and convex hull, the effect of such noises is reduced, and the algorithm becomes robust and correctly segments the eye from fish images.

One more significant contribution of the proposed work is its computational efficacy. The imaging techniques used in proposed work are computationally efficient. This makes the algorithm fast and capable of detecting the changes introduced in samples due to exposure to heavy metal. The transformation and representation of these discriminatory changes are presented using a very low computation parameter, *i.e.* angle subtended by an arc at the centre of a circle, makes the process suitable for real time applications.

2. Materials and methods

2.1. Fish collection and acclimatization

Fresh water fish *Chana punctatus* were procured from fish farm with average wet weight and length of 20 ± 2.0 g m, 12 ± 0.5 cm, respectively. All fishes were acclimatized in glass aquaria (50 L Capacity) in dechlorinated water at laboratory conditions (24 ± 2 °C) for 15 days. Fishes were fed with goat liver during acclimatization, as these fishes are primarily carnivorous in nature and Mercury level in goat liver as par the various scientific studies [1]-DOI:10.1080/02652030802566319) is also expected to be very low. Heavy metal (Mercuric chloride, 99.5%) for present study was procured from Fisher Scientific. Water used during the study was free from prior trace of any heavy metals.

2.2. Experimental procedure

Post-acclimatization, fishes were divided into two groups. First group of fishes were exposed with mercuric chloride (0.10 mg/l), and second group was maintained as control (no metal exposure). The dosage of mercuric chloride was selected based on LC50 analysis (sublethal dose). Fishes were exposed to metal for 15 days. Some earlier studies [3,4], reported significant elevations in liver antioxidant enzymes from the 7th day onward and maintained until the 15th day after this it again started to decrease. Hence based on these data, the fishes were exposed with metals for 15 days.

Daily renewal of water as well as metal was done to maintain the concentration of metal in tanks. Fishes were fed with goat liver during experiment. Both groups contained five fishes with 20 L of water in each aquarium. Experiment was performed in triplicates. There was no mortality during exposure period.

2.3. Sample preparation

After 15 days, fishes from each aquarium were taken out and anesthetized by immersing in aqueous solution (25 mg/l) of tricaine methane suffonate (MS 222) for 3–5 min. Fishes thereafter were preserved for imaging study in thermocol boxes with fish to ice ratio of 1:2.

2.4. Image acquisition set up

Images of fish samples were captured using a self-developed image acquisition system. Samples were illuminated using three fluorescent tube-lights (length of 2 feet), four CFLs (25 W) and 3 LED lamps. These light sources were used as they emit white light. The lamps and CFLs were placed at the walls and corners of a cuboid shaped wooden box to give a uniform light intensity over the fish sample while the LED lamps were used to eliminate the shadow generated due to camera placed above the fish sample. Images were captured using a colour digital camera placed vertically above the sample at an approximate distance of 10 cm. A point and shoot digital camera of 8-MP with auto focus has been used for image acquisition. The camera rendered images in JPEG format of resolution 5184*3888 pixels. The angle between the camera lens axis and the lighting sources was around 45°. Fig. 1 shows the

Fig. 1. Image acquisition setup.

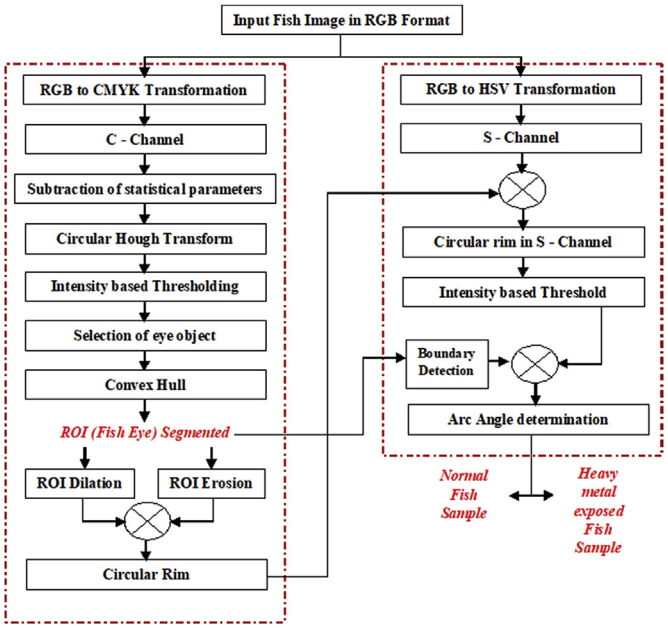

Fig. 2. Block Diagram of the techniques used in the proposed work.

image acquisition setup used to capture image for image processing.

3. Analysis of fish samples for determination of a visual identifier using computer vision analysis

The proposed work deals with an unconventional, non-destructive and completely automated computer vision analysis of fish samples when exposed to heavy metals like mercury. The proposed work also deals with determining a ***potential visual feature*** which can be speculated and used for differentiation of a normal fish used in the proposed work from a heavy metal exposed fish. Fishes were exposed with mercuric chloride (0.10 mg/l) for 15 days.

Computer vision techniques seem to be an optimum choice for analysis of visual changes that occur in the body parts of the fish samples when exposed to mercury. Due to its non-destructive behaviour, computational efficiency, real-time analysis and automated decision making, computer vision techniques have been used in the proposed work for classification of heavy metal treated fish samples from normal ones.

Fig. 2 shows the block diagram of image processing techniques used in the proposed work. Some visual changes around the eye-balls of fish samples are observed when exposed to heavy metals. In the proposed work, the eye-balls have been considered as region-of-interest (ROI) and are segmented to study the features corresponding to visual changes occurring in treated fish samples. Due to the presence of some artefacts created during the image acquisition process, that might affect the segmentation accuracy, the input images have been transformed to different colour spaces. Due to the circular shape of ROI, the colour space transformed images are subjected to Circular Hough Transform (CHT). CHT is capable of detecting circles in an image. Once the eye-balls are segmented, its positional and geometrical features are determined in the form of centre and radius, respectively. These features are used to segment a concentric rim around the periphery of eye-ball for analysing the changes occurring in treated fish samples. The discriminatory changes have been translated and represented using a mathematical parameter, which is used in identifying a fish sample as normal or heavy metal exposed.

The entire proposed methodology can be divided into two main parts:

a Segmentation of Region-of-Interest
  i Colour space transformation, channel selection and pre-processing
  ii Circular Hough Transform
  iii Binarizing the pre-processed image and selecting the Region-of-Interest
  iv Post-processing of segmented Region-of-Interest
b Identification of a potential visually dicriminatory feature and translating it to mathematical parameter

3.1. Segmentation of Region-of-interest

3.1.1. Colour space transformation, channel selection and pre-processing

The captured images of fish samples are in coloured RGB format. During the image acquisition of fish samples, some artefacts like reflections occur in images which might hamper the accuracy of the algorithm for segmentation of ROI. Apart from artefacts, various body parts of fish may possess similar characteristics as eye-ball and act as noise. Hence, the input image in coloured RGB format is not analysed in its present form and is transformed into a different colour space for segmentation of ROI. Out of the many colour spaces, CMYK colour space has shown favourable characteristics for segmentation of eye-balls. The C-channel from CMYK colour space creates a distinction between the ROI and background pixels. Hence, this channel is considered for ROI segmentation.

Fig. 3 shows the input image and its constituting channels for a sample fish image. Fig. 3(a) shows input RGB image which constitutes of front part of the fish body captured from a lateral view. The image consists of reflection artefacts in the eye and on the body of the fish.

Fig. 3. Input Image and its decomposition (a) Input image in RGB format (b) Red Channel (c) Green Channel (d) Blue Channel.

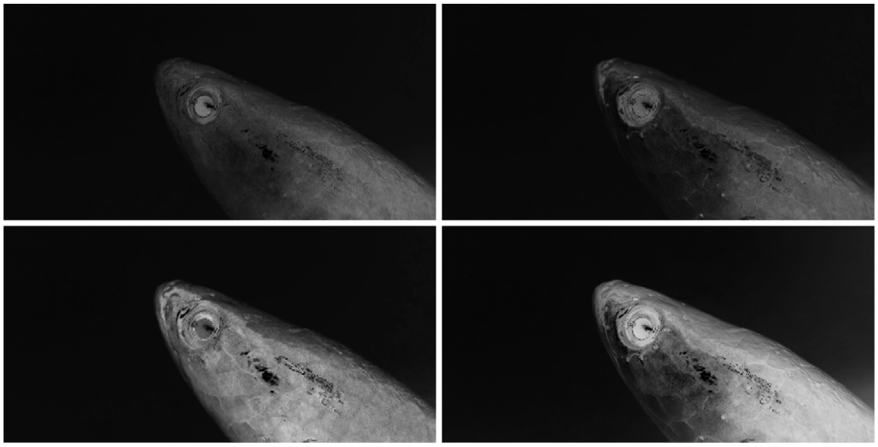

Fig. 4. CMYK Transformation and its decomposition (a) C-Channel (b) M-Channel (c) Y-Channel (d) K-Channel.

Table 1
Comparison of pixel intensities in original and preprocessed image.

S No	Pixel Intensity Level	Image	
		Original Image	Pre-processed Image
1	0	0	0
2	mean + std	m + s	0
3	a	a	a - m - s
4	255	255	255 - m - s

Fig. 3(b) and (c) and 3(d) shows the individual channels, namely, red, green and blue, respectively. It can be observed that the eye ball is not clearly discriminatory in any of the 3 channels and hence, a colour transformation is needed.

Fig. 4 shows the individual channels of input image transformed to CMYK colour space. The C-channel shows a discrimination in ROI and background pixels and has been considered for segmentation. Other channels are rejected as they don't have any clear discrimination between pixels.

The transformation of an image from RGB-to-CMYK colour space takes place with the help of mathematical equations which are summarized in Algorithm 1 [29]:

Algorithm 1. RGB to CMYK colour space transformation

Step-1 Load input image in RGB format.
Step-2 Extract individual channels of input image and store them as R, G and B.
Step-3 The individual channels of RGB image are normalised by dividing each pixel value by 255.

$$R1 = R/255 \quad (1)$$

$$G1 = G/255 \quad (2)$$

$$B1 = B/255 \quad (3)$$

Step-4 Now, the individual channels of CMYK colour space are determined.
Step-5 K-channel of CMYK image is determined as follows:

$$K = 1 - \max(R1, G1, B1) \quad (4)$$

Step-6 C-Channel is determined as follows:

$$C = (1 - R1 - K)/(1 - K) \quad (5)$$

Step-7 M-channel is determined as follows:

$$M = (1 - G1 - K)/(1 - K) \quad (6)$$

Step-8 Y-channel is determined as follows:

$$Y = (1 - B1 - K)/(1 - K) \quad (7)$$

C–channel seems optimum and is considered for segmentation of ROI from the sample images. The ROI appears to be one of the brightest regions in this image and is subjected to a pre-processing step [14,15,27]. Since, the ROI pixels are super pixels and have high intensities, so, to create further discrimination of ROI pixels from the background, the mean and standard deviation of the image is determined, summed up together and subtracted from the original C-channel image. Mathematically, the pre-processed image is obtained as follows and the new image will have updated pixel intensities as summarized in Table 1.

$$I_{new} = C - \text{mean}(C) - \text{std}(C) \quad (8)$$

3.1.2. Circular Hough Transform

The ROI, i.e. the eye-balls, in the image is almost circular in shape or has some portion which may be considered part of circle. Circular Hough Transform (CHT) is a computation technique used for detection of circles from imperfect or noisy digital images. A 2-dimensional mathematical representation of a circle of radius R and centre (a, b) is given as:

$$(x-a)^2 + (y-b)^2 = R^2 \quad (9)$$

The parametric space conversion of the above equation is given as:

$$x = a + R*\text{Cos}(\theta) \quad (10)$$

$$y = b + R*\text{Sin}(\theta) \quad (11)$$

If radius, R, is known then some points can be found in x-y space which will lie on the circumference of the circle or will satisfy eqn (9). Now, these points in the image are transformed to a Hough parameter space, i.e. a-b space. A circle is drawn for each point identified in x-y space with (x, y) as centre and radius, R. A point in the a-b space common to all the circles drawn, is ultimately identified as the centre and taken back to the x-y space to locate a circle with centre (a,b) and radius, R [12]. This is graphically represented in Fig. 5.

Since, the ROI is circular in shape, hence, CHT has been employed for detection of circles in the pre-processed image. A range of empirical values of the radius is given as input to the CHT algorithm and it finally results in the detection of a circle centre with specified radius value from the image. In the proposed work, the CHT algorithm is brute forced and is run iteratively by changing threshold, until a circle is detected in the image.

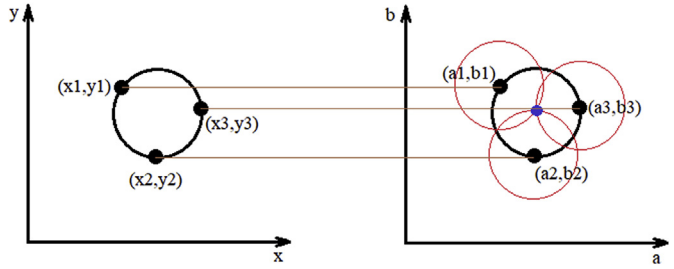

Fig. 5. Space Transformation for implementation of Circular Hough Transform.

The CHT algorithm is directly dependent on the radius of the circle to be detected. In the proposed work, the radius for detection of eye in the images is chosen to be greater than 30 pixels for an image resolution of 1354 * 684 pixels. In case, there is change in the image resolution, the radius for detection can be altered by using following formula:

$$R_{new} = R * \min((W_{new} / W), (H_{new} / H))$$

Where, reference image resolution = W * H (used in proposed method).New image resolution = W_{new} * H_{new}New radius for circle detection = R_{new}W, H = width and height of the reference image, respectively.Wnew, Hnew = width and height of the new image, respectively.

3.1.3. Binarizing the pre-processed image and selecting the ROI

The pre-processed image obtained earlier, is binarized to segment ROI from the input image. The pre-processed grayscale image is converted to a binary image using an adaptive threshold. The local statistical parameters from the image under test are determined and combined strategically to determine a threshold which converts the image into binary image, provided the ROI is clearly detected. The statistical parameters used in determining the thresholds are mean and standard deviation. Some, weights have been assigned to both parameters which have been determined empirically, after analysing many input images. The threshold for binarization is as follows:

$$Th_{ROI} = w1*std(p) + w2*mean(p) \quad (12)$$

Where, w1 and w2 are the weights assigned and their values are 1 and 4 respectively.p is the pre-processed image.

Post binarization, it can be observed that some pixels, corresponding to reflection artefacts, inside ROI are not segmented. Hence, a binary hole-filling operation is applied on the resulting binary image.

3.1.4. Post-processing of segmented ROI

The reflections that might occur during the image acquisition process are usually bright in colour and might be present either at the periphery or inside the eye region. As it can be observed that the segmented ROI does not have a complete boundary and some portion is missing due to the reflection pixels. In order to obtain an exact object corresponding to ROI, the resulting image is subjected to a convex hull operation. A convex hull is a set of pixels in the spatial domain which can enclose the entire object. If the boundary pixels of the eye breaks due to such reflection pixels, then the convex hull connects the corners of the broken boundary and addresses this problem.

3.2. Identification of the potential visually discriminatory feature and translating it to mathematical parameter

Once, the ROI is detected and segmented, the next step comes in observing the discriminatory visual changes that occur in fish samples when exposed to heavy metals. In the proposed work, there has been a novel and unique observation which has become the root cause to consider the eye region for analysis. It has been observed that there are some visual changes near the periphery of the eye balls in fish images. It may be due to accumulation of mercury in and around the eyes and the inflammation [24]. This phenomenon causes changes in the colour of skin near the eye region. So, in order to analyse and demonstrate this change, this observation is considered as a potential and vital information and translated to mathematical parameters.

It has been observed that due to the increase in blood concentration near the eye when exposed to heavy metals, the region becomes brownish. Although, for a normal fish sample, this region is limited to a quadrant. But it extends to a semi-circular region or may be more for a treated fish. So, to represent these changes, this brown region is segmented from grayscale image of a colour space transformed image. A concentric circular rim is created around the segmented ROI, and intensity-based threshold is applied to segment the brown coloured region. Since, the region is located on the periphery of a circular region, hence, the feature are translated to a mathematical entity and represented in form of angle subtended by an arc.

The changes observed in the fish samples are distinguishable in saturation channel of HSV colour space. So, initially, the input image is transformed to HSV colour space and saturation channel is extracted and used for further processing. Fig. 6 shows the colour space transformed image and its decomposition. The transformation is done using some standard mathematical equations, which are summarized as Algorithm 2 [29].

Algorithm 2. RGB to HSV Colour Space Transformation

Step-1 Load input sample image in RGB format.
Step-2 Transform the image to HSV format using following

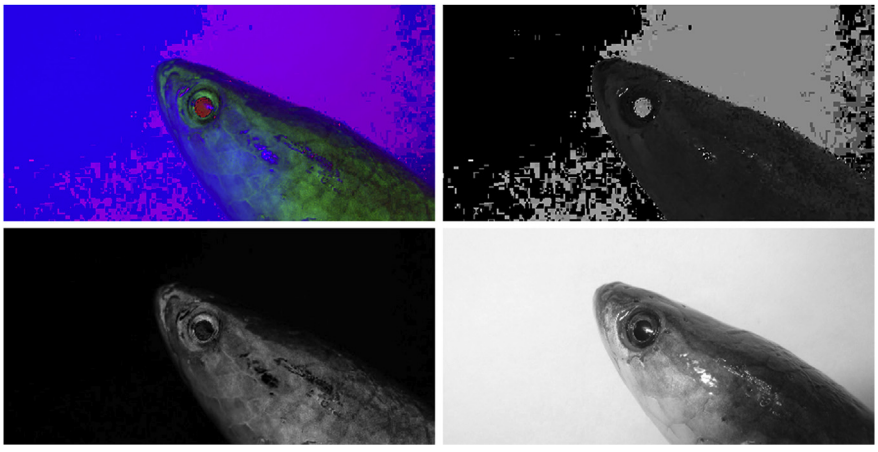

Fig. 6. RGB to HSV Colour space transformation (a) HSV Image (b) H-channel (c) S-channel (d) V-channel.

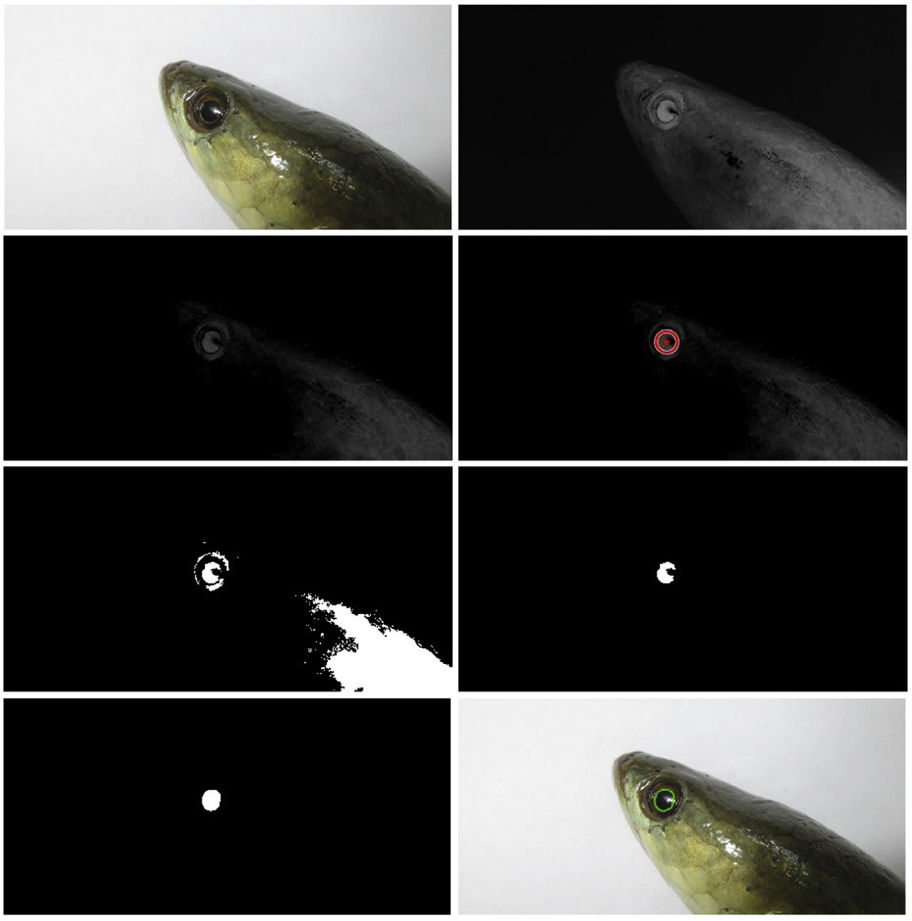

Fig. 7. Segmentation of ROI (a) Sample Input Image (b) Original C – channel Image (c) Pre-processed C - channel Image (d) Pre-processed image marked with detected circle and its centre obtained using CHT (e) Binary Image with multiple objects (f) Binary image with ROI segmented (g) Convex Hull of segmented ROI (h) Boundary of convex hull marked on input image.

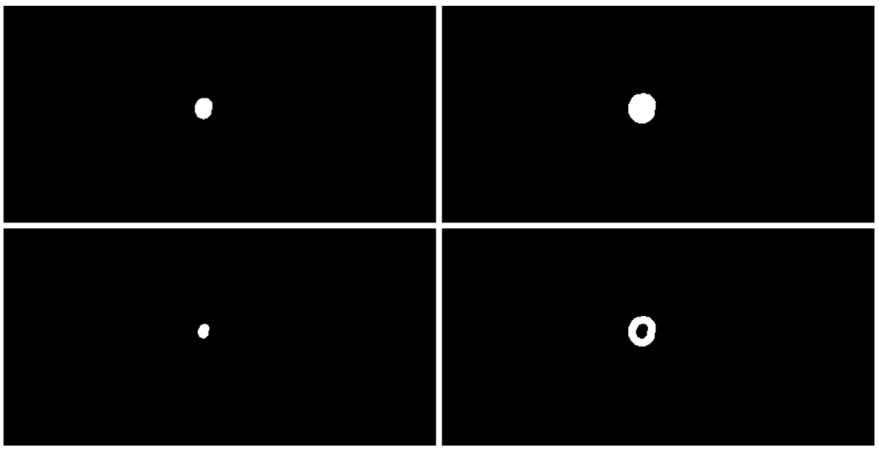

Fig. 8. Creation of concentric rim (a) Segmented ROI (b) Dilated ROI (c) Eroded ROI (d) Circular Rim.

transformation equations:

The intensity values for individual channel of input image is normalised as follows:

$$R1 = Rr/255 \tag{13}$$

$$G1 = Gg/255 \tag{14}$$

$$B1 = Bb/255 \tag{15}$$

The maximum, minimum and their difference is calculated as follows:

$$Cmax = \max(R1,G1,B1) \tag{16}$$

$$Cmin = \min(R1,G1,B1) \tag{17}$$

$$Delta = Cmax - Cmin \tag{18}$$

Values for Hue channel are calculated as follows:

$$H = \begin{cases} 60° \times \left(\frac{G1 - B1}{Delta}\ mod 6\right), & Cmax = R1 \\ 60° \times \left(\frac{B1 - R1}{Delta} + 2\right), & Cmax = G1 \\ 60° \times \left(\frac{R1 - G1}{Delta} + 4\right), & Cmax = B1 \end{cases} \tag{19}$$

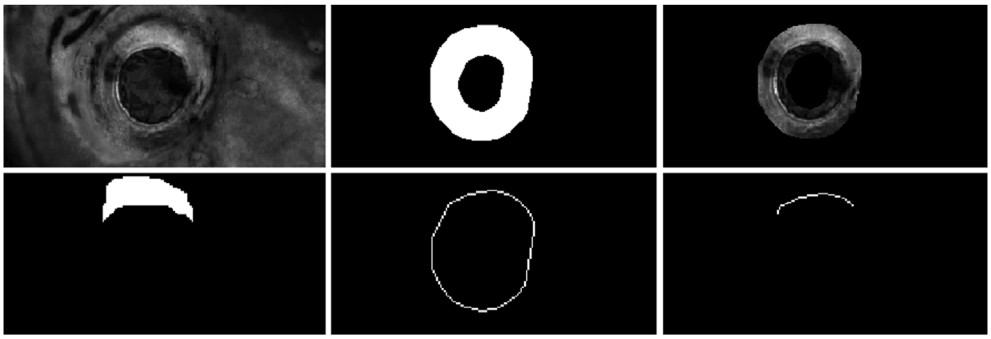

Fig. 9. Translation of discriminatory feature to mathematical parameters (a) Saturation channel of the fish image (b) Circular Rim in binary format (c) Binary circular rim multiplied with saturation channel (d) Intensity based threshold to obtain potentially discriminatory region (e) Boundary of the segmented ROI (f) Region common to ROI and potentially discriminatory region.

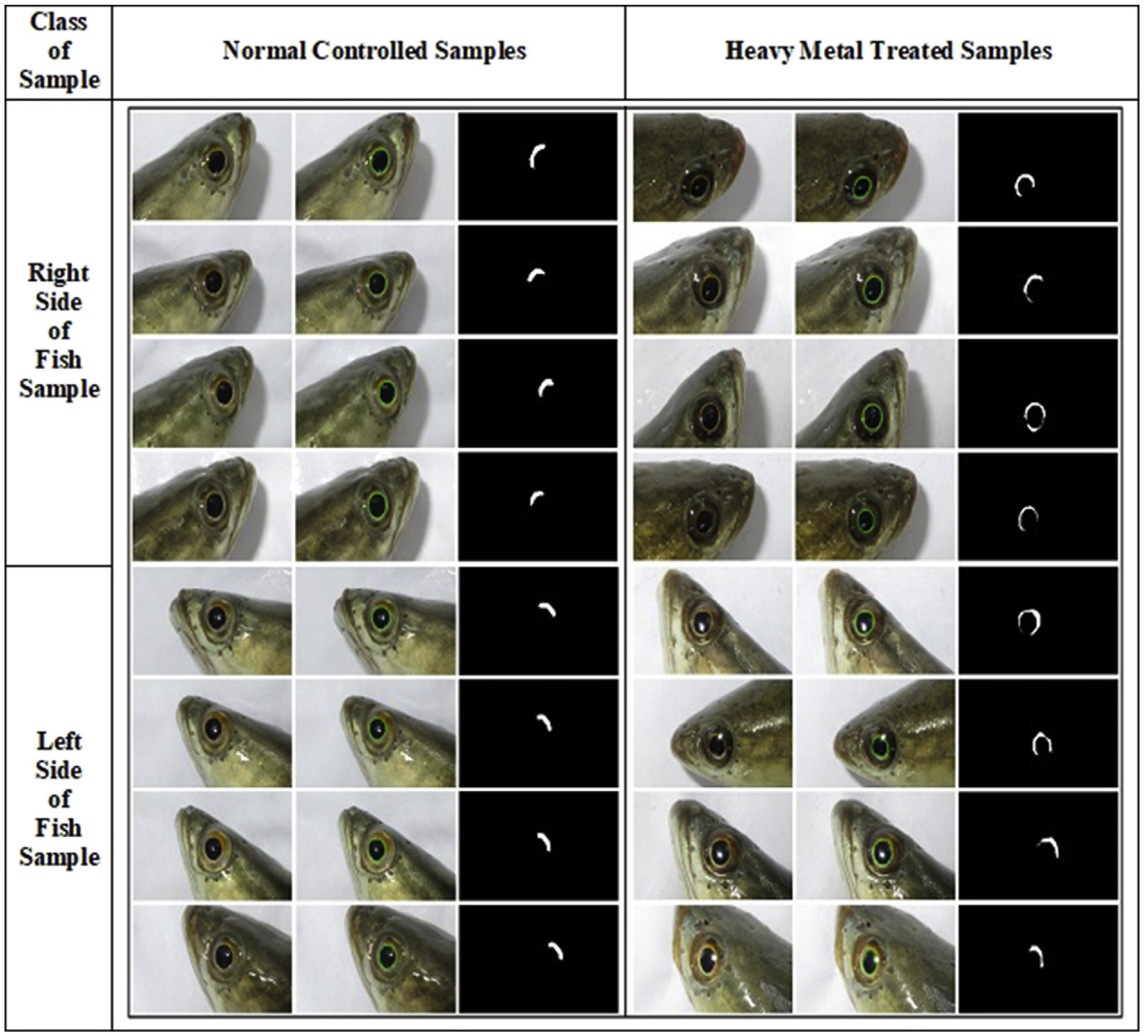

Fig. 10. Experimental Results (a) Input fish image in RGB format (b) Fish image marked with boundary of segmented ROI with green colour (c) Visually discriminatory region to differentiate both fish classes identified in a sample.

Values for Saturation channel are calculated as follows:

$$S = \begin{cases} 0, & Cmax = 0 \\ \frac{Delta}{Cmax}, & Cmax \neq 0 \end{cases} \quad (20)$$

Values for Value channel are calculated as follows:

$$V = C_{max} \quad (21)$$

Step-3 Consider the saturation channel for further processing.

Geometrical features such as centre and radius of the segmented ROI are determined and used to construct a concentric circular rim which will be used for potential feature identification. For creation of this rim, the finally obtained ROI is subjected to some mathematical morphological operations. Initially, the ROI is dilated by a disc shaped structuring element of size 10 pixels and then eroded by a disc structuring element of 5 pixels and then the eroded image is subtracted from dilated image. This results in a binary image consisting of the rim.

The rim acts as a mask for segmentation of feature region and is multiplied with the saturation channel. The resultant image is subjected to intensity-based thresholding to finally obtain the visual feature. The boundary pixels of this region are obtained and the common region between ROI boundary and rim boundary pixels is determined. Finally,

Table 2
Discriminatory feature values for samples of both classes.

S No	Treated		Normal	
	Left	Right	Left	Right
1	132.73	235.64	80.66	122.13
2	167.45	225.12	84.21	101.74
3	207.54	212.00	76.11	120.68
4	165.63	142.50	14.08	14.00
5	128.77	173.47	44.25	82.50
6	149.34	286.53	76.98	27.00
7	129.09	234.90	76.36	113.68
8	201.06	192.09	77.94	72.15
9	130.00	223.13	71.59	48.00
10	144.63	215.17	53.65	27.12
11	174.83	200.00	90.00	120.73
12	233.10	205.51	52.00	112.26
13	156.04	140.21	70.11	81.23
14	179.37	144.22		
15	201.35	195.51		
16	233.21	206.43		

the length of this region is determined by summing up the number of white pixels in resulting image. The sum of white pixels is considered as length because the intersection of boundary pixels in both images is of single pixel width. Next, the circumference of ROI is determined in a similar way. Finally, angle subtended by the arc is determined and used as a feature for discrimination of a treated fish from a normal one. The angle subtended is determined as follows:

$$Angle = \left(\frac{Arc - length}{Circumference}\right) \times 360° \quad (22)$$

Mathematically, the entire process is summarized in Algorithm 3.

Algorithm 3. Translation of Visually Discriminatory Feature to Mathematical parameters

Step-1 Determine the centre and radius of the eye segmented from fish sample.
Step-2 Obtain image I_d and I_c by performing morphological dilation and erosion operation on binary image of fish eye.
Step-3 Subtract the eroded image from the dilated, to obtain rim around fish eye as follows:

$$I_{rim} = I_d - I_e$$

Step-4 Perform a pixel-wise multiplication of the binary image of rim with the saturation channel of input sample image.
Step-5 The resultant image is subjected to an automated intensity-based thresholding with threshold value as follows:

$$Th = 0.6*\max(I_{rim}*I_{saturation})$$

Step-6 The boundary pixels of segmented fish eye are obtained and multiplied with the thresholded image.
Step-7 Length of common area both to the rim and eye boundary is determined by counting the number of white pixels.
Step-8 The biomarker is converted to mathematical parameter by evaluating the angle subtended by an arc at the centre of circle.
Step-9 Angle subtended by an arc is derived as follows:

$$Angle = (Length\ of\ arc)/(Circumference\ of\ circle)$$

4. Experimental Results

The proposed algorithm has been tested on a database which consists of fish images belonging to normal and heavy metal treated class. A total of 116 fish samples were sampled for the experimentation, which consisted of samples belonging to both classes. All samples have been photographed from left and right side. From the sample fish images, the eyes are located using Circular Hough Transform and segmented using intensity-based thresholding. Post-segmentation, a circular rim around the eye is segmented and subjected to intensity threshold to determine some potential visual feature which discriminates between samples of both classes. Finally, the discriminatory feature is transformed into mathematical parameters and a threshold is determined to differentiate between both classes.

Fig. 7 shows the result of segmentation of the eye ball region from the input fish image. The input image in RGB format is first converted to CMYK channel, whose C-channel is used for further processing. The C-channel is subjected to a pre-processing step to highlight the eye region in the full image. This process highlights brighter pixels and removes pixel with low intensities, thereby, shifting the origin from a zero-pixel intensity to arithmetic sum of mean and standard deviation. Fig. 7(a) shows a sample input image and Fig. 7(b) show the C-channel in which the eye region is visible as pixels with high intensities. Fig. 7 (c) shows the pre-processed image from which the local features have been subtracted to highlight the region of interest. This process makes

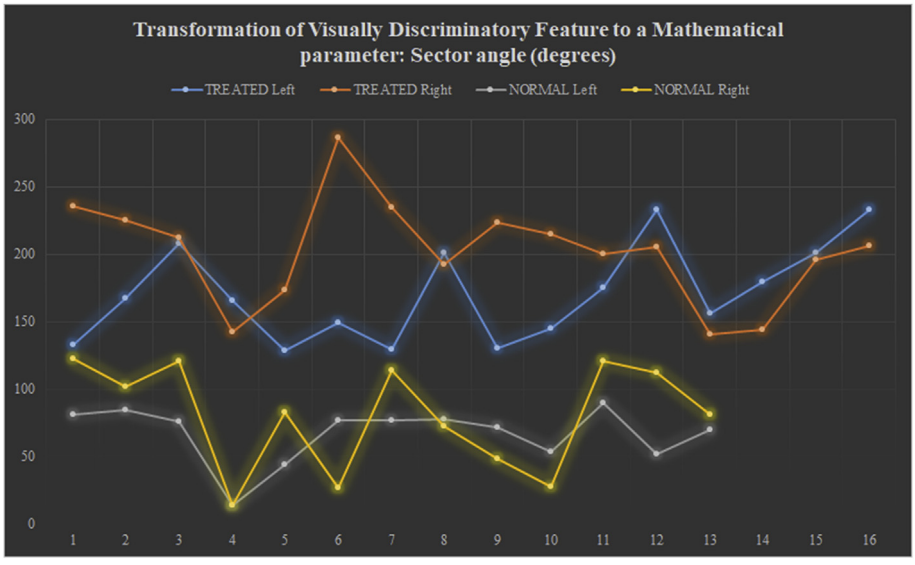

Fig. 11. Scatter plot of the values of the discriminatory feature values obtained for samples from both classes.

Table 3
Computation time (IN seconds) elapsed in ROI segmentation, circular rim creation and visually discriminatory feature region translation

Computation Time (seconds)									
S No	Fish Sample	Left Side of fish sample				Right Side of fish sample			
		ROI Segmentation	Rim Creation	Feature Translation	Total Time	ROI Segmentation	Rim Creation	Feature Translation	Total Time
1	**Normal**	1.8556	0.0391	0.0635	**1.9581**	1.9077	0.0404	0.0499	**1.9979**
2	**Controlled**	1.8668	0.0384	0.0545	**1.9597**	1.7923	0.0379	0.0547	**1.8848**
3	**Samples**	1.7342	0.0378	0.0570	**1.8291**	1.9706	0.0388	0.0540	**2.0634**
4		1.7769	0.0379	0.0542	**1.8689**	1.8176	0.0372	0.0537	**1.9085**
5		1.7383	0.0318	0.0547	**1.8248**	1.8428	0.0320	0.0564	**1.9312**
6		1.8704	0.0315	0.0541	**1.9560**	1.8140	0.0312	0.0503	**1.8955**
7		1.7226	0.0310	0.0544	**1.8080**	1.8890	0.0312	0.0536	**1.9738**
8		1.6823	0.0311	0.0529	**1.7663**	1.8936	0.0312	0.0503	**1.9751**
9		1.6726	0.0310	0.0519	**1.7554**	1.7256	0.0289	0.0490	**1.8036**
10		1.7661	0.0309	0.0515	**1.8484**	2.0301	0.0310	0.0525	**2.1137**
11		1.7091	0.0294	0.0489	**1.7874**	1.8089	0.0311	0.0496	**1.8897**
12		1.8353	0.0317	0.0523	**1.9193**	1.7613	0.0308	0.0529	**1.8449**
13		1.8203	0.0310	0.0507	**1.9020**	1.8907	0.0306	0.0500	**1.9714**
14	**Heavy**	1.9943	0.0399	0.0538	**2.0880**	1.9606	0.0410	0.0516	**2.0532**
15	**Metal**	2.3841	0.0398	0.0536	**2.4775**	1.8815	0.0399	0.0535	**1.9750**
16	**Treated**	2.9615	0.0406	0.0512	**3.0533**	1.8537	0.0410	0.0555	**1.9501**
17	**Samples**	1.7250	0.0391	0.0536	**1.8177**	1.9291	0.0385	0.0521	**2.0198**
18		1.7017	0.0381	0.0487	**1.7885**	1.8551	0.0316	0.0538	**1.9404**
19		1.8737	0.0392	0.0488	**1.9616**	1.5829	0.0316	0.0556	**1.6701**
20		2.6108	0.0317	0.0550	**2.6975**	1.7617	0.0310	0.0519	**1.8445**
21		1.6066	0.0318	0.0561	**1.6945**	1.8586	0.0313	0.0525	**1.9424**
22		3.3070	0.0304	0.0495	**3.3869**	1.8198	0.0315	0.0508	**1.9020**
23		1.7794	0.0311	0.0512	**1.8617**	2.1481	0.0307	0.0524	**2.2313**
24		1.8254	0.0313	0.0513	**1.9080**	1.8277	0.0320	0.0503	**1.9100**
25		1.8007	0.0316	0.0535	**1.8859**	2.0297	0.0307	0.0549	**2.1152**
26		1.8204	0.0311	0.0517	**1.9032**	1.8901	0.0318	0.0519	**1.9738**
27		1.8809	0.0308	0.0498	**1.9615**	1.8491	0.0315	0.0512	**1.9318**
28		1.7482	0.0313	0.0510	**1.8304**	1.9977	0.0287	0.0500	**2.0764**
29		1.8691	0.0317	0.0531	**1.9539**	2.0844	0.0316	0.0525	**2.1684**

the algorithm adaptive and image independent. The pre-processing step is helpful in removing some redundant information from the image, thereby, increasing computational efficacy of the algorithm. Fig. 7(d) shows the result of CHT implementation. The CHT algorithm has been used to detect a centre in the image. Since, the eye ball is almost circular in shape, hence, it is subjected to CHT. The CHT algorithm gives the radius and centre of the detected circle as its output. The sample image with circle detected and its centre marked in red colour on the image is shown. Fig. 7(e) shows the binary image of the pre-processed C-channel image. This is achieved using adaptive Otsu's threshold. It can be observed that multiple objects have been segmented and obtained in the binary image. This is where, the centre detected using CHT comes handy and is used to select the object corresponding to ROI. Fig. 7(f) shows the binary image containing only the ROI selected using the centre obtained from CHT algorithm. Fig. 7(g) shows the finally segmented ROI pixels in binary image. Since, due to reflection artefact the eye region was not correctly segmented during the threshold operation, hence, a convex hull operation was performed to complete the boundary of the segmented region. Fig. 7(h) shows the boundary points of segmented ROI marked on input RGB image in green colour.

Fig. 8 shows the result of rim created for a sample image. Fig. 8(a) shows the segmented ROI obtained after convex hull operation. This ROI is subjected to morphological operations, such as dilation and erosion. Finally, a strategic subtraction is performed using both operations to obtain a rim around the eye region. Fig. 8(b) shows a dilated rim image while Fig. 8(c) shows an eroded rim image. Fig. 8(d) shows the final rim obtained by performing the subtraction using above images.

Fig. 9 shows the results of the process to determine the angle subtended by the arc. The region is clearly distinguishable from the other regions near the eye in saturation region. Hence, the image in RGB format has been converted to HSV format and its S-channel has been used for arc determination. Fig. 9(a) shows the saturation channel which is cropped near the eye region. Fig. 9(b) shows the circular rim, obtained earlier, in binary image. The cropped S-channel image and binary image are multiplied and subjected to intensity based threshold operation. Fig. 9(c) and (d) shows the results of multiplication and threshold operation, respectively. Fig. 9(e) shows the boundary obtained of the threshold rim image while Fig. 9(f) shows the discriminatory feature region reduced to single pixel width.

Fig. 10 shows the results of eye segmentation and visually discriminatory region, used to differentiate between both fish classes under consideration, for that image. The results are shown for a few samples from both classes, namely, normal and heavy metal treated. Fig. 10(a) shows the input image under test. The input image is a colour image in RGB format. This image is subjected to a colour space transformation, i.e. RGB-to-CMYK transformation, and its C-channel is further used for eye region detection and segmentation using Hough Transform and intensity thresholding. Fig. 10(b) shows the boundary of the eye region segmented using proposed algorithm. Another colour space transformation, i.e. RGB-to-HSV transformation, takes place and S-channel is used for visually discriminatory feature determination. Fig. 10(c) shows the visually discriminatory region for differentiating a normal from a heavy metal treated fish sample, identified in the image in binary format.

This visually discriminatory feature is converted to a mathematical parameter, sector angle, whose values are presented in Table 2. The table consists of these values for all samples used for experimentation purpose. Clearly, it can be observed that there is a considerable difference in the range of values for both classes. The values of the sector angle for both sides, i.e. left and right, of the heavy metal treated fish samples are observed to be greater than its counterpart. For the samples under experimentation, the value of sector angle for normal samples lies in the range 14–122°. However, for treated samples, the samples are

Table 4
FISH freshness and pesticide detection models using image processing.

S No	Paper	Objective	Features Used	Results	Computation Time
1	Hyman, [13]	Identify fish freshness and quality	Gills	A monotonous decline in the feature value as the retention time increases.	3 s
2	Kumar et al. [17]	Identify fish quality after pesticide exposure	Gills	95% accuracy has been achieved in correctly classifying a fish for presence of pesticide or not.	2.5 s
3	Hu et al. [30]	Recognition of infected fish species	Skin	Identification any infection on basis of colour and texture of fish skin has been reported.	Not reported
4	Siddiqui et al. [31]	Fish species classification using deep learning	Convolutional feature maps of fish	Classification of 94.3% for a dataset of 16 fish species.	Not reported
5	Sengar et al. [32]	Identify fish quality post exposure to pesticides present in water	Eye	97% accuracy achieved in correctly identifying fish samples with pesticide present.	1.5 s
6	Qin et al. [33]	Underwater live fish recognition	Convolutional feature maps	98.64% accuracy achieved for fish recognition using deep learning	Not reported
7	Salman et al. [34]	Fish species classification in underwater environment	Species dependent visual features	90% accuracy achieved in using correctly identifying fish species.	Not reported
8	Issac et al. [35]	Identify fish freshness	Gills	98% accuracy achieved using the developed framework	3.5 s
9	Allken et al. [36]	Identify fish species using synthetic data	Convolutional feature maps	94% accuracy achieved in using correctly identifying fish species.	Not reported
10	Proposed Work	Classification of heavy metal treated fish	Eye	Arc near eye region identified due to oxidation process which is validated by the ground truth.	1.99 s

observed to have a higher value and lies in the range 128–286°. If a value close to 125° is taken as threshold, then it can act as an optimum threshold for differentiating the given samples.

A visual representation of the above observation is represented graphically in Fig. 11. The samples belonging to treated class are shown in orange and blue colour while those belonging to the normal class are shown with the help of yellow and grey colour. It is clear from the scatter plot that treated samples have high value as compared to the normal ones.

The time elapsed for segmentation of eye region and conversion of the identified feature to mathematical parameter is tabulated in Table 3. The proposed work was done in MATLAB R2016b (Math Works) software on a CPU@ 2.3 GHz, 4 Gb RAM, 64-bit operating system. An average time of 1.99 s is elapsed in complete analysis and determination of a test sample as normal or treated using proposed methodology.

A comparison of the proposed work has been done with different papers which have already been published in the field of fish analysis using computer vision techniques is reported in Table 4. From the table, it can be observed that most of the work has been done in the field of fish species classification using imaging and machine learning approach. Some work has been done in the field of freshness and quality assessment post exposure to pesticides. Some work has been reported in the field of quality assessment of fish samples from harvesting to selling period. The proposed work seems novel and no such work has been reported which considers the analysis of exposure of heavy metals on fish samples using computer vision techniques.

5. Discussions

The proposed work is a preliminary study which involves the use of computer vision techniques to identify some visual changes in a heavy metal exposed fish. Such visual changes can be used as indicative parameters for the customers to identify some aberrations in a fish sample. Fishes are consumed across the globe by humans. However, due to the contamination of water bodies, the accumulation of unnatural agents may occur in the body of the fish. When such fishes are consumed by humans, they may pose a threat to the well being of humans.

The use of imaging techniques has become very common to provide a solution to many real-time problems which have some visual discrimination in normal and under treated conditions. Due to its non-destructive behaviour, computational efficiency, real-time analysis and automated decision making, computer vision techniques have been used in the proposed work for classification of heavy metal treated fish samples from normal ones. Although, to start with, the results obtained using computer vision needs to be validated against the results obtained from the traditional approaches or against the ground truth.

For validation purpose, the dataset used in the proposed work has been labelled with classes (heavy metal treated or untreated) and used as ground truth to check the performance of the proposed algorithm. The fishes that were exposed to heavy metals were grouped and labelled as one class while the untreated samples were labelled as the other class. This ground truth helped in validating if a particular sample under test belonged to which class. The smaller value of the sector angle obtained belonged to the untreated class while larger value corresponded to the heavy metal treated class. This validation approach has been used in the proposed work.

It has been reported in literature that the heavy metals may cause oxidative stress in the fish samples which can be correlated to the melanin synthesis. From the experimentation performed in the proposed work, it has been observed that the region surrounding the eye shows some visual changes which can potentially be vital in classifying a fish sample as normal or heavy metal treated. The conversion of this feature into mathematical parameter has shown that the feature value is more for a heavy metal treated fish sample as compared to a normal one. This can be justified by the fact that free radical generated due to

oxidative stress caused by heavy metal exposure stimulate the hyper production of melanin pigment. In addition, the skin around the eye is delicate and thin. Change in blood flow due to stress also have an impact on this particular area and the effect of melanin production is more visible near the eye region.

This current approach may be used for other heavy metals such as As, Cd, Pb, etc and may also get similar results and the biomarker can be applicable for all fish species. However, the intensity of the effect may vary across the fish species as well as the heavy metal under consideration. More studies will be required for confirmation before establishing any conclusion.

6. Conclusions

The objective of the proposed work is to identify a visual identifier for fish samples *(channa punctatus)* which are exposed with heavy metals *(Hg)*. A computer vision method has been proposed in this work because of its computational strength and non-destructive nature. Following points can be concluded on the basis of the proposed study:

a Out of the many factors which can determine the quality of a fish sample, parameters belonging to the appearance class have been considered as there are some visual changes in fish samples on exposure to heavy metals. The parameter used in the proposed work is the fish eye region.
b The eye region is segmented properly and correctly by using preprocessing, Circular Hough Transform and adaptive intensity threshold. The combination of these imaging techniques along with mathematical morphological operations, like convex-hull, the algorithm is able to correctly overcome the issues related to reflections which are been introduced during the image acquisition process. The algorithm has become robust to illumination conditions.

The algorithm is computationally efficient and can be a first step to identify the presence of heavy metals with the help of a visual identifier in fish samples.

Conflicts of interest

None.

References

[1] E. Adei, K. Forson-Adaboh, Toxic (Pb, Cd, Hg) and essential (Fe, Cu, Zn, Mn) metal content of liver tissue of some domestic and bush animals in Ghana, Food Addit. Contam. B 1 (2) (2008) 100–105, https://doi.org/10.1080/02652030802566319.
[2] D. Albores-Garcia, L.C. Acosta-Saavedra, A.J. Hernandez, M.J. Loera, E.S. Calderón-Aranda, Early developmental low-dose methylmercury exposure alters learning and memory in periadolescent but not young adult rats, BioMed Res. Int. (2016) 12–16 2016.
[3] T. Allen, S.V.S. Rana, Effect of arsenic (AsIII) on glutathione-dependent enzymes in liver and kidney of the freshwater fish *Channa punctatus*, Biol. Trace Elem. Res. 100 (2004) 39–48.
[4] P.S. Basha, A.U. Rani, Cadmium-induced antioxidant defense mechanism in freshwater teleost *Oreochromis mossambicus* (Tilapia), Ecotoxicol. Environ. Saf. 56 (2003) 218–221.
[5] P. Boffetta, E. Merler, H. Vainio, Carcinogenicity of mercury and mercury compounds, Scand. J. Work. Environ. Health 19 (1) (1993) 1–7.
[6] L.A. Broussard, C.A. Hammett-Stabler, R.E. Winecker, J.D. Ropero-Miller, The toxicology of mercury, Lab. Med. 33 (8) (2002) 614–625.
[7] M.K. Dutta, A. Issac, N. Minhas, B. Sarkar, Image Processing based Method to assess fish quality and freshness, J. Food Eng. 177 (2016) 50–58.
[8] M.K. Dutta, N. Sengar, N. Kamble, K. Banerjee, N. Minhas, B. Sarkar, Image processing based technique for classification of fish quality after cypermethrine exposure, LWT - Food Sci. Technol. (Lebensmittel-Wissenschaft -Technol.) 68 (2016) 408–417.
[9] Y. Fakhri, N. Saha, A. Miri, M. Baghaei, L. Roomiani, M. Ghaderpoori, M. Taghavi, H. Keramati, Z. Bahmani, B. Moradi, A. Bay, R.H. Pouya, Metal concentrations in fillet and gill of parrotfish (Scarus ghobban) from the Persian Gulf and implications for human health, Food Chem. Toxicol. 118 (2018) 348–354.
[10] X. Feng, S. Tang, L. Shang, H. Yan, J. Sommar, O. Lindqvist, Total gaseous mercury in the atmosphere of Guiyang, PR China, Sci. Total Environ. 304 (2003) 61–72.
[11] I. Galvin, C. Alonso-Alvarez, An intracellular antioxidant determines the expression of a melanin-based signal in a bird, PLoS One 3 (2008) e 3335.
[12] H. Rhody, Lecture 10: Hough Circle Transform, (Oct. 2005).
[13] M. Hyman, The impact of mercury on human health and the environment, Altern. Ther. 10 (6) (2004) 70–75.
[14] A. Issac, M. Parthasarthi, M.K. Dutta, An adaptive threshold based algorithm for optic disc and cup segmentation in fundus images, 2nd International Conference on Signal Processing and Integrated Networks (SPIN), 2015, pp. 143–147 Noida.
[15] A. Issac, M. ParthaSarathi, M.K. Dutta, An adaptive threshold based image processing technique for improved glaucoma detection & classification, Comput. Methods Progr. Biomed. 122 (2) (2015) 229–244.
[16] F. Kroon, C. Streten, S. Harries, A protocol for identifying suitable biomarkers to assess fish health: a systematic review, PLoS One 12 (4) (2017) e0174762 http://doi.org/10.1371/journal.pone.0174762.
[17] P. Kumar, Y. Prasad, A.K. Patra, D. Swarup, Levels of cadmium and lead in tissues of freshwater fish (*Clarias batrachus L.)* and chicken in western UP (India), Bull. Environ. Contam. Toxicol. 79 (2007) 396–400.
[18] W.C. Li, H.F. Tse, Health risk and significance of mercury in the environment, Environ. Sci. Pollut. Res. 22 (2015) 192–201.
[19] P.N. Manavi, A. Mazumder, Potential risk of mercury to human health in three species of fish from the southern Caspian Sea, Mar. Pollut. Bull. 130 (2018) 1–5.
[20] N.B. Metcalfe, C. Alonso-Alvarez, Oxidative stress as a life-history constraint: the role of reactive oxygen species in shapingphenotypes from conception to death, Funct. Ecol. 24 (2010) 984–996.
[21] J. Moreno, P. Møller, Are melanin ornaments signals of antioxidant and immune capacity in birds? Curr. Zool. (Acta Zool. Sin.) 52 (2006) 202–208.
[22] A.G.M. Osman, A.M.A. Reheem El, K.Y. AbuelFadl, A.G. GadEl-Rab, Enzymatic and histopathologic biomarkers as indicators of aquatic pollution in fishes, https://doi.org/10.4236/ns.2010.211158, (2010) 2 11 1302 1311.
[23] W. Ouyang, Y. Wang, C. Lin, M. He, F. Hao, H. Liu, W. Zhu, Heavy metal loss from agricultural watershed to aquatic system: a scientometrics review, Sci. Total Environ. 637–638 (2018) 208–220.
[24] R. Pereira, E. Leite, J. Raimundo, S. Guilherme, Só Puga, M.A. Santos, Canário Joã, A. Almeida, Má Pacheco, Patrí Pereira, Metals(loids) targeting fish eyes and brain in a contaminated estuary - uncovering neurosensory (un)susceptibility through bioaccumulation, antioxidant and morphometric profiles, Mar. Environ. Res. 140 (2018) 403–411.
[25] J. Rahmani, Y. Fakhri, A. Miri, A. Shahsavani, Z. Bahmani, M.A. Urbina, S. Chirumbolo, H. Keramati, B. Moradi, A. Bay, G. Bjørklund, A systematic review and meta-analysis of metal concentrations in canned tuna fish in Iran and human health risk assessment, Food Chem. Toxicol. S0278–6915 (18) (2018) 30397-1.
[26] Ribeiro C.A.de O, A. Katsumiti, P. França, J. Maschio, E. Zandoná, M.M. Cestari, T. Vicari, H. Roche, H.C.S. de Assis, F.F. Neto, Biomarkers responses in fish (Atherinella brasiliensis) of paranaguá bay, southern Brazil, for assessment of pollutant effects, Braz. J. Oceanogr. 61 (1) (2013) 1–11.
[27] M. Soorya, A. Issac, M.K. Dutta, An image processing algorithm for automated and robust Glaucoma Diagnosis from fundus images using novel blood vessel tracking and bend point detection, Int. J. Med. Inform. 110 (2018) 52–70 Feb 2018.
[28] F. Zahir, S.J. Rizwi, S.K. Haq, R.H. Khan, Low dose mercury toxicity and human health, Environ. Toxicol. Pharmacol. 20 (2005) 351–360.
[29] A. Ford, A. Roberts, Colour space conversions. *Technical Report* Westminster University, 1998 (London).
[30] J. Hu, D. Li, Q. Duan, G. Chen, X. Si, Preliminary design of a recognition system for infected fish species using computer vision, CCTA 2011, Part I, IFIP AICT 368 (2012) 530–534.
[31] S.A. Siddiqui, A. Salman, M.I. Malik, F. Shafait, A. Mian, M.R. Shortis, E.S. Harvey, Automatic fish species classification in underwater videos: exploiting pre-trained deep neural network models to compensate for limited labelled data, ICES (Int. Counc. Explor. Sea) J. Mar. Sci. 75 (2018) 374–389.
[32] N. Sengar, M.K. Dutta, B. Sarkar, Computer vision based technique for identification of fish quality after pesticide exposure, Int. J. Food Prop. 20 (2017) 2192–2206.
[33] H. Qin, X. Li, J. Liang, Y. Peng, C. Zhang, DeepFish: accurate underwater live fish recognition with a deep architecture, Neurocomputing 187 (2016) 49–58.
[34] A. Salman, A. Jalal, F. Shafait, A. Mian, M. Shortis, J. Seager, E. Harvey, Fish species classification in unconstrained underwater environments based on deep learning, Limnol Oceanogr. Methods 14 (2016) 570–585.
[35] A. Issac, M.K. Dutta, B. Sarkar, Computer vision based method for quality and freshness check for fish from segmented gills, Comput. Electron. Agric. 139 (2017) 10–21.
[36] V. Allken, N.O. Handegard, S. Rosen, T. Schreyeck, T. Mahiout, K. Malde, Fish species identification using a convolutional neural network trained on synthetic data, ICES J. Mar. Sci. (2018), https://doi.org/10.1093/icesjms/fsy147.